European Journal of Chemistry

Journal webpage: www.eurjchem.com

Design, synthesis and characterization of MOF-199 and ZIF-8: Applications in the adsorption of phenols derivatives in aqueous solution

Liliana Giraldo [1], Marlon Bastidas-Barranco [2], Pablo Húmpola [3] and Juan Carlos Moreno-Piraján [4,*]

[1] *Facultad de Ciencias, Universidad Nacional de Colombia, Bogotá, 11001000, Colombia*
[2] *Facultad de Ingeniería, Grupo DestaCar, Universidad de la Guajira, Guajira, 440001, Colombia*
[3] *Facultad de Bioquímica y Cs. Biológicas, Universidad Nacional del Litoral, Santa Fe, 3000, Argentina*
[4] *Facultad de Ciencias, Grupo de Investigación en Sólidos Porosos y Calorimetría, Universidad de los Andes, Bogotá, 11001000, Colombia*

** Corresponding author at: Facultad de Ciencias, Grupo de Investigación en Sólidos Porosos y Calorimetría, Universidad de los Andes, Bogotá, 11001000, Colombia. Tel.: +57.1.3394949. Fax: +57.1.3394949. E-mail address: jumoreno@uniandes.edu.co (J.C. Moreno-Piraján).*

ARTICLE INFORMATION

DOI: 10.5155/eurjchem.8.3.293-304.1603

Received: 28 June 2017
Received in revised form: 05 August 2017
Accepted: 05 August 2017
Published online: 30 September 2017
Printed: 30 September 2017

KEYWORDS

ZIF-8
Phenols
MOF-199
Microporous
Metal-organic framework
Adsorption characteristics

ABSTRACT

In this work, the adsorption characteristics of metal-organic frameworks (MOFs: MOF-199 and ZIF-8) with two different types of structure were analyzed. MOF-199 consists of copper-based metal clusters while the ZIF-8 consists of organic molecules interlaced with zinc atoms and these have octahedral morphology and typical rhombic dodecahedron shape, respectively. The results of phenol (Ph) and *p*-nitro phenol (PNP) adsorption capacity from aqueous solution show that MOF-199 has a higher adsorption capacity: Ph 79.55% and PNP 89.3%, while for ZIF-8 the adsorption capacity was Ph 65.5% and PNP 77.0%. Adsorption of phenols was fit to Langmuir, Sips and Redlich-Peterson models and kinetics by pseudo-second order. Gibbs free energy (ΔG°) shows that adsorption processes studied are spontaneous.

Cite this: *Eur. J. Chem.* **2017**, *8(3)*, 293-304

1. Introduction

With the passing of years and constant progress of industrial processes, many beneficial systems for the everyday wellbeing of humanity have been developed. However, these same industrial progresses have been very aggressive with the environment by causing alterations; as an example, we can mention climate change, an effect that should be solved from the basic sciences. This effect is caused by a combination of factors including indiscriminately disposing into rivers, lakes and water highly dangerous pollutants that alter the balance of ecosystems. Among the many pollutants we mention the two, with which this research will deal with: phenol and *p*-nitro phenol [1-12].

Phenolic compounds are a family of organic compounds that serve the chemical industry and are often used as intermediates in synthesis processes of other compounds (e.g. production of pharmaceuticals, pesticides, dyes, artificial resins, explosives, and other valuable fine chemicals) [1-6,13], and many industries and particularly in developing countries, do not perform proper treatment prior to disposal, but the "remove" without treatment and are thrown to the water which may subsequently come in contact with living beings causing serious problems to the environment and health.

Phenolic compounds are highly toxic compounds and once discarded without pretreatment, intermediate reactions that produce other by-products which are not bio-degradable naturally, such as particularly the phenol and *p*-nitrophenol [1,14-19], which cause methemoglobin formation, anemia, liver and kidney damage, eye and skin irritation, tumor formation, cancer, and systemic poisoning [20-24]. As a result, both phenol and *p*-nitrophenol has been categorized as one of the 126 priority pollutants by the US Environmental Protection Agency (US EPA) [13-25]. Therefore, fast and effective removal of phenolics compounds from wastewater is becoming more and more urgent.

In order to confront these problems and eliminate particularly such compounds several methodologies have been raised that have undoubtedly resulted in several valid cases. Among them it is worth mentioning cases reported in the literature such as adsorption [4-15,26], oxidation [19-29], membrane separation [20-26], and extraction [24-29]. Among these technologies, adsorption is recognized as the most applicable one for single-design, easy-operation, and high-efficiency [18,25-27] and in the adsorption process, activated

ISSN 2153-2249 (Print) / ISSN 2153-2257 (Online)
http://dx.doi.org/10.5155/eurjchem.8.3.293-304.1603

carbon is popularly employed as adsorbent for its large specific surface area and high adsorption capacity [1,3,4,8,17,28]. Even though activated carbon material is considered one of the best materials to solve environmental pollution problems, it has limitations including poor mechanical strength and difficult-regeneration [3,26,28,29].

Therefore there is a growing interest in this area of adsorption to develop materials that can have a good adsorption capacity and further comply with other requirements as high mechanical strength, high reusability, and ready availability, especially the adsorbent based on the naturally occurring materials for their ready availability and excellent biocompatibility Which will not cause additional environmental pollution during their application.

For this reason, in this research we decided to analyze some new type of porous network material named Metal Organic Frameworks (MOFs), which has attracted great attention among the scientific community [29-32]. These materials are synthesized by combining metal ions and organic ligands to form a porous crystalline network. With their exceptional physical and chemical properties, MOFs have had a significant impact on disciplines related to gas storage and adsorption [30,33-35], catalysis [30,36-38], drug delivery [35,39], and sensing [40]. Recently, a number of studies started to evaluate the feasibility of MOFs to remove contaminants from water such as metal ions [30,41], dyes [42], and other organic compounds [30,43], revealing that MOFs can be stable in the aqueous environment and exhibit great capacity to separate the targeted contaminants.

Therefore the scope of this work is to prepare MOF's (MOF-199 and ZIF-8) and evaluate its adsorption capacity of phenol (Ph) and *p*-nitrophenol (PNP). To achieve this goal the MOFs were characterized by Fourier transform infrared spectroscopy (FT-IR), X-ray diffraction (XDR), thermogravimetric analysis (TGA), scanning electron microscopy (SEM), point of zero charge (PZC), influence of pH, adsorption isotherm of N_2 and CO_2. Isotherms in aqueous solution were determined and six theoretical models are applied to establish which fits best for the adsorption of phenols on MOFs. A kinetic and thermodynamic study was realized to establish the adsorption mechanism of phenols on MOFs and energetic character.

2. Experimental

2.1.1. Synthesis of MOF-199

MOF-199 was prepared by a modification of the synthesis procedure described in the literature [44-47]. In a typical preparation [45], a solid mixture of $Cu(NO_3)_2{\cdot}3H_2O$ (0.654 g, 2.22 mmol) and 1,3,5-benzenetricarboxylic acid (H_3BTC) (0.326 g, 1.55 mmol) was dissolved in a mixture of DMF (3 mL), ethanol (4 mL) and water (2 mL) in a 20 mL vial. The vial was heated at 85 °C in an isothermal oven for 48 h, yielding light blue crystals. After cooling the vial to room temperature, the solid product was obtained by decanting from the mother liquor and washed with DMF (4 mL × 9 mL). Solvent exchange was then carried out with ethanol (4 mL × 9 mL) at room temperature. The product was then dried under vacuum (at ≤ 5 mTorr overnight) at 170 °C for 8 h, yielding 0.345 g of MOF-199 during which time, the deep blue solid became blue-violet [44].

2.1.2. Synthesis of ZIF-8

ZIF-8 was synthesized at room temperature following a slightly modified method presented in the literature [48]. In this paper, 1.467 g of $Zn(OAc)_2$ and 25.670 g 2-methylimidazole were first dissolved in 10 g and 100 g deionized water, respectively. The two solutions were then mixed under stirring at room temperature (25±1 °C). The molar ratio of Zn^{2+}: 2-methylimidazole:H_2O in the mixture was of 1:75:1260. After 10 min of stirring, the product was collected by centrifugation at 10000 rpm for 45 min, and then washed with Ultrapure deionized (DI) water (18 MΩ·cm, Millipore) for several times. The obtained ZIF-8 were dried in an oven at 80 °C for 24 h to remove residual water and then kept in a desiccator for use.

2.2. Computational details

Initially the MOF-199 and ZIF-8 were modeled from structures unitary the Cambridge Crystallographic Data Center. These structures are optimized classically using molecular mechanics method with force field AMBER and the energies being considered: bond, angle bond, dihedral, van der Walls, electrostatic and hydrogen-bonden. The algoritm of the geometric optimization was Steepest descent (RMS gradient 0.1 kcal Å/mol and 1785 maximum cycles). The optimized calculations were performed using Hyperchem 8.0.10 molecular modeling program [49-53].

2.3. Textural characterization of MOF's

The textural preliminary characterization of materials was performed by physical adsorption of N_2 at 77.4 K using an Autosorb IQ2 Quantachrome Instruments. The results of the gas-solid isotherms were analyzed in different ranges of pressures, using the BET method on which calculation of specific surface (p/p^0 range determined using the method proposed by Rouquerol *et al.* ([54,55], Dubinin-Astakhov (DA) for the analysis of micropores (p/p^0 range < 0.1) and the volume of narrow micropores, pores < 0.7 nm, was calculated by applying DA equation to the CO_2 adsorption data at 0 °C and density functional theory (p/p^0 range 1×10^{-7}-1.0) considering different pores models and the effects of surface roughness and heterogeneity (NLDFT and QSDFT), using software ASQiWin [54].

2.4. Infrared spectroscopy of MOF's

FT-IR absorbance spectra of the metal-organic frameworks were obtained through KBr technique, with the analysis performed on a Nicolet™ iS™50 FT-IR spectrometer in the wave number range of 4000-400 cm^{-1}. The solid samples were mixed with KBr at a ratio of roughly 1/300, and then the mixture was ground in an agate mortar to very fine powder. After drying at 100 °C for 12 h in a vacuum oven, about 300 mg of the fine powder were used to make a pellet. After preparation, the pellet was analyzed immediately and the spectra were recorded by 32 scans with 4 cm^{-1} resolution. A pellet prepared with an equivalent quantity of pure KBr powder was used as background.

2.5. SEM-EDX of the metal-organic framework (MOF's)

To analyses of the morphology, chemical composition, and the elemental maps of the samples were conducted by a JEOL JSM-7100FA field emission scanning electron microscope equipped with an energy dispersive X-ray (EDX) system.

2.6. Adsorption equilibrium experiments of phenol's on the metal-organic framework

Phenol and 4-nitrophenol (Sigma-Aldrich Co, USA) were used as probe molecules for to assay their removal using the metal-organic framework (MOF's) synthesized in this research (MOF-199 and ZIF-8) (labeled in this work as Ph for phenol and PNP for 4-nitrophenol). Table 1 shows various properties of phenols used. The adsorption experiments were conducted in a batch mode.

Table 1. Properties of phenol and 4-nitrophenol.

Property	Phenol	4-Nitrophenol
Molecular weight (g/mol)	94.11	139.11
pKa	9.95	7.16
Solubility (g/L) at 293.15 K	83.11	16.00
Width (Å)	6.38	6.70
Length (Å)	7.92	8.45
Thickness (Å)	8.22	8.93
UV analysis (nm)	269.50	400.00
Dipole moment/D	1.22	5.70

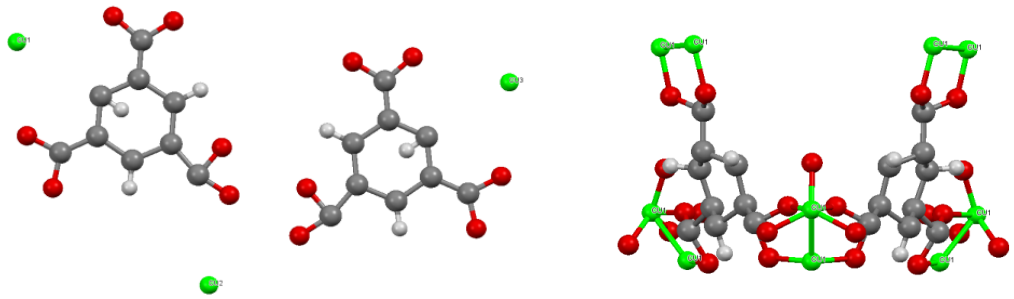

Figure 1. Geometry optimization on structure of MOF-199.

First, different amounts of metal-organic framework (MOF-199 and ZIF-8) were put into several 250 mL flasks, which contained 100 mL of phenol solution (500 mg/L). Then, the flasks were kept in a rotary shaker (200 rpm) under isothermal conditions (298.15 K) for a week to give enough time to achieve the equilibrium state. Prior to UV measurement, all of samples were filtered for the separation of metal-organic framework present in phenols solutions. The concentration of the filtrate was determined by an UV spectrometer (Shimadzu UV-160A, Japan) at 269.5 nm for phenol and 400 nm for 4-nitrophenol. The adsorption capacity of metal-organic framework at the equilibrium state was calculated as follow:

$$q_e = (C_o - C_e)\, V/W \quad (1)$$

where q_e is the adsorbed amount (mg/g), C_o is the initial concentration of phenol (mg/L) (or 4-nitrophenol) and C_e is equilibrium concentration (mg/L). V and W are the volume of the solution (L) and the mass of an adsorbent used (mg), respectively.

2.7. Determination of point of zero charge (pH_{pzc}) an effect of pH on the adsorption capacity in phenols-MOFs system

A study to determine the effect of initial pH on the adsorption capacity of phenols was performed. For this the solution pH set from 3 to 12, while the amount of adsorbent (0.05 g), volume of solution (200 mL), initial concentration of solution (100 mg/L), temperature (303.15 K) and shaker speed (200 rpm) were kept constant. The solution pH was adjusted by using diluted 0.1 M HCl and 0.1 N NaOH. The amount adsorbed during the adsorption was calculated, as given in the Section 2.6.

Previously the point of zero charge (pH_{pzc}) was determined. Quantities of the MOFs weighed in a range from 0,050 to 0,300 g, in an interval of 0.05 g approximately. Each of the heavy materials was placed in vials of 15 mL is added to each 10 mL of sodium chloride solution (0.1 N NaCl). The vials were closed and left under constant stirring at a temperature of 298 K for 48 hours. The samples were centrifuged at 3000 rpm for 15 minutes and the supernatant is removed using a 0.2 micron Whatman filter. Subsequently the pH of each of the filtered supernatants in a pH meter Schott TitroLine alpha plus was measured. The pH of each sample based on its weight is plotted, and the point of zero charge is determined as the pH at which the curve tends to all the samples in suspension.

2.8. Kinetic studies

All the phenols kinetic experiments were carried out at 298.15 K and this study was performed by varying the initial concentration of the phenols solution. Initially, the metal-organic framework (MOF's) was added into a glass vessel, which contained 2 L of phenol or 4-nitrophenol solutions. The experiments were conducted for 8 h in a water bath, while the phenols solution was stirred at constant speed under isotherm condition. During the kinetic experiments, the phenol solution (10 mL) was taken out and filtered at pre-determined time intervals to measure the remaining phenols concentration in the glass vessel. Then, the solution concentration of the filtrate was calculated as described in the Section 2.6 [56], and finally the results were analyzed using various models to establish the mechanism of adsorption between the adsorbate and adsorbent.

3. Results and discussion

3.1 Structure of MOFs

Geometry optimization on structure of MOF-199 and ZIF-8 given in Figure 1 and 2.

3.2. N_2 and CO_2 adsorption isotherms analysis for MOF-199 and ZIF-8

The morphological properties of MOF-199 and ZIF-8 were determined by nitrogen sorption analysis at 77.4 K. The adsorption isotherms correspond to type I, according to the IUPAC classification, Figure 3. The isotherms of adsorption-desorption of the materials prepared in this work reflects the microporous network (pore size < 2 nm) of ZIF-8. Further inspection of the low-pressure region of the adsorption isotherm shows that ZIF-8 has slight change in the trend of the isotherm corresponding to type VI behavior. Some authors in the literature have discussed this phenomenon as a consequence of gas induced structural flexibility of the ZIF-8 frameworks or weak interaction between the adsorbate-adsorbent.

Table 2. DA and DFT parameters obtained from the adsorption-desorption isotherm of N_2 at 77.4 K.

Samples	S_{BET}	DA (P/P^0< 0.1)				DFT (P/P^0 10^{-7}-1)	
	[m^2/g^{-1}] *	V_{mic} [cm^3/g]	E_o [Kj/mol]	n	Pore Radius [Å]	V_P [cm^3/g]	Half Pore Width [Å]
MOF-199	2271	0.66	8.47	3.4	7.0	0.69	3.5
ZIF-8	2266	0.88	4.47	3.4	8.6	0.65	4.6

* Value range corrected as p/p° optimum (Rouquerol *et. al.*, 2007, [80]).

Table 3. Mean error adjustment between different surface textures (NLDFT vs. QSDFT) in pores slit and slit/cylindrical.

Sample	NLDFT		QSDFT	
	Fitting error (slit pore) [%]	Fitting error slit (cylindrical pore) [%]	Fitting error (slit pore) [%]	Fitting error slit (cylindrical pore) [%]
MOF-199	0.60	0.14	0.84	0.70
ZIF-8	4.43	5.45	3.34	2.73

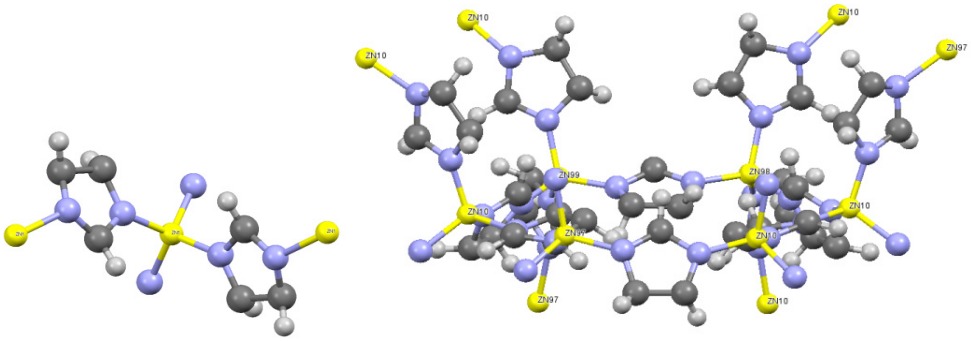

Figure 2. Geometry optimization on structure of ZIF-8.

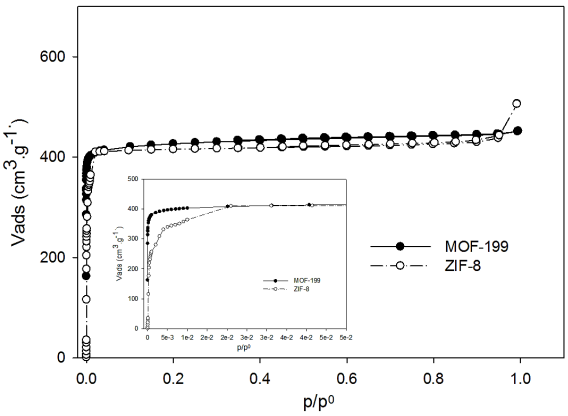

Figure 3. The N_2adsorption-desorption isotherms MOF-199: filled circle and ZIF-8: hollow circle.

Between these authors Yaghi [57], Fairen-Jimenez [58], and Webley [59] have also reported this interesting phenomenon. The microporous volume is 0.88 $cm^3.g^{-1}$ calculated by the application of the DA method. The synthesized sample is a microporous material with a BET specific surface area with 2266 m^2/g (calculated relative pressure from 0.009 to 0.02).

The textural properties of the synthesized materials are summarized in Table 2.

The results show that the two synthesized materials in this study have a high BET specific surface area (Brunuer-Emmett-Teller) [60-63], even higher than those reported in the literature for such materials; this is probably because of the small changes carried out during the synthesis process which have a direct influence on the way networks are armed and therefore the generation of pores. The parameters other if different being higher for the MOF-199 for ZIF-8 as e.g. micropore volume where for MOF-199 is 0.66 and for ZIF-8 0.88 cm^3/g, as are higher parameters other as E_o (characteristic energy, E_o), radius pores, pore volume and average pore size. In this paper we want to elaborate a little in the evaluation of the distribution of pore size by functional theory density, because the reports in scientific literature are not many in this area, so we proceeded to compare the theoretical isotherms obtained for NLDFT and QSDFT models (Non Local Density Functional Teory and Quenched Solid Density Functional Theory respectively) for different pore shapes vs the experimental isotherms [62]. The results show in Table 3.

QSDFT, contrary to NLDFT, best fits the experimental data adjustments of ZIF-8, possibly due to the presence of roughness and chemical and/or geometric in the pore wall heterogeneities. However, the error is large and the theoretical isothermal presents greater dispersion, especially at low pressures (See Figure 4). This indicates that there can be more pronounced heterogeneity in smaller pores.

MOF-199 shows a suitable fit with a model homogeneous pore walls by the method (NLDFT). As shown in Figure 5 and due to the marked microporosity of samples, it was proposed for further information, the analysis at low pressures using the Dubinin-Astakhov model (see Figure 6).

Table 4. DA parameters obtained from the adsorption isotherm of CO_2 to 273.15 K.

	DA (CO_2)			
	V_{mic}[cm^3/g]	E_o [Kj/mol]	n	Pore radius [Å]
MOF-199	2.91	4.53	1.3	8.2
ZIF-8	5.19	1.85	1.0	10.6

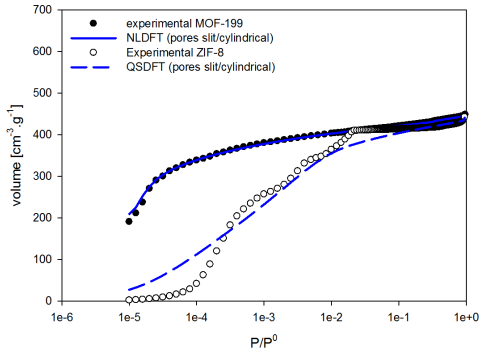

Figure 4. Analysis of the porosity applying, NLDFT and QSDFT for MOF's synthesized: MOF-199/NLDFT and ZIF-8/QSDFT.

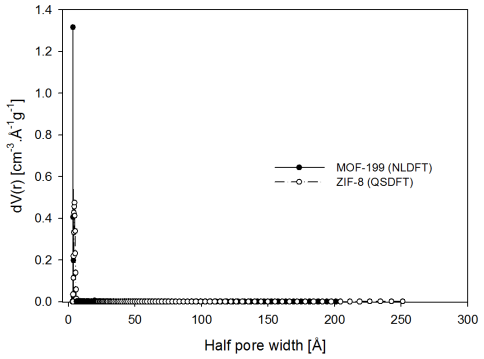

Figure 5. Porosity analysis: a) MOF-199: filled circle and b) ZIF-8: hollow circle.

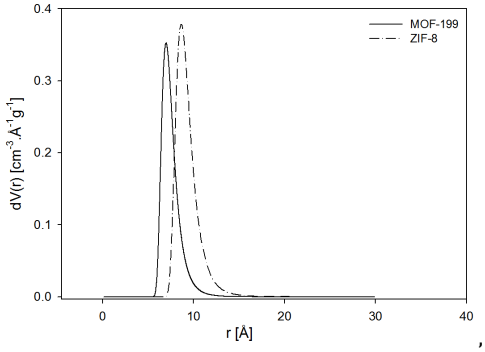

Figure 6. Size distribution of pores of MOF-199 and ZIF-8 from the N_2 adsorption isotherms at 77.4 K. The Weibull equation was used for analysis of DA at low pressures.

It can be seen that while most V_{mic} presents ZIF-8 (Table 2, the characteristic energy into the micropores is vastly superior in MOF-199 (this term, with the BET surface condition the slight difference in favor observed in N_2 adsorption).

The parameter n of the Dubinin-Astakhov equation [63] provides a measure of the description of the adsorption data in many microporous solids, ranging from a narrow (n~3) to a wide (n < 3) micropore size distribution. In this manner and in line with that observed in the plot, a close micropore size distribution (see n~3 in Table 4).

In order to provide more complete information on the presence of micropores smaller not detected by the N_2, it is proposed to extend the investigation by adsorption of CO_2 at 273.15 K, because it is sensitive to inaccessible micropores N_2 to 77.4 K.

The adsorption equilibrium isotherms for CO_2 at 273.15 K for MOF-199 and the ZIF-8 were further determined from o to 0.030 in relative pressure (P/P^0), this in order to avoid the problems by the nitrogen at cryogenic temperatures, allowing adsorbate to enter the narrow microporosity [62,64], are represented graphically in Figure 7. MOF-199 presents a major adsorption capacity versus ZIF-8 probably due to morphological and chemical differences. On the other hand the analysis was performed porous narrow from the isotherms of CO_2, Figure 7.

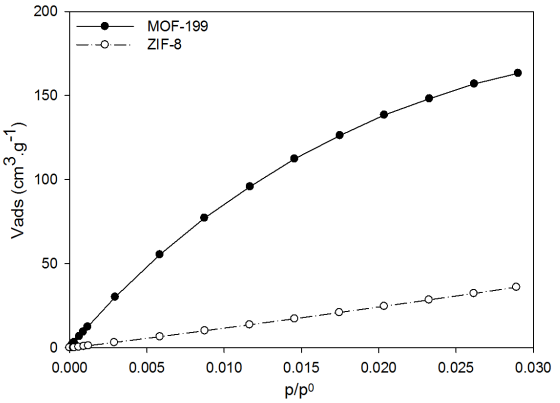

Figure 7. Adsorption-desorption isotherms of CO_2 to 273.15 K. a) MOF-199: filled circle and b) ZIF-8: hollow circle.

The data analysis CO_2 adsorption to 273.15 K using DA (Dubinin-Astakhov), shows that there are (closer) smaller micropores with a wide distribution of sizes (n < 3). The CO_2 adsorption isotherm at 273.15 K, shows that for MOF-199 enhanced CO_2 adsorption capacity, possibly associated with increased energy characteristic in the pores. Furthermore, ZIF-8 shows a trend in the size distribution curve of larger pores, indicating greater heterogeneity (see Figure 8).

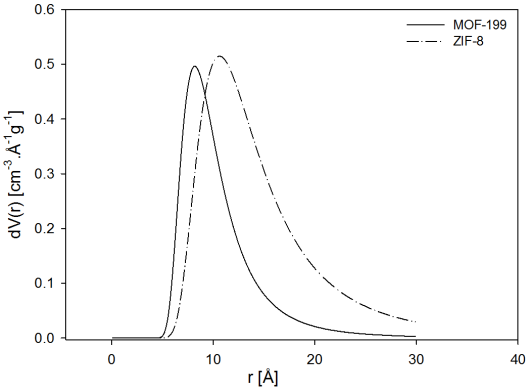

Figure 8. Size distribution of pores of MOF-199 and ZIF-8, from CO_2 adsorption isotherms at 273.15 K.

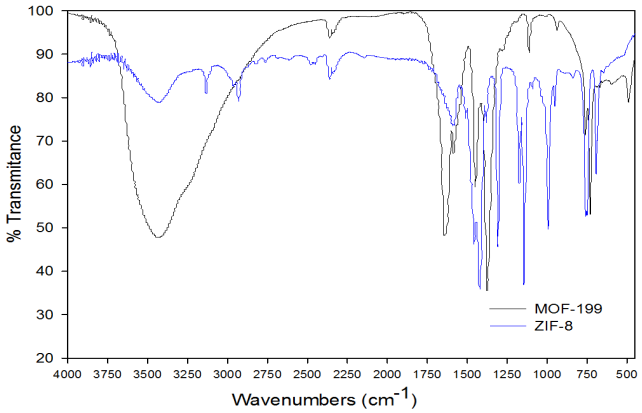

Figure 9. FT-IR spectra of MOF-199 and ZIF-8.

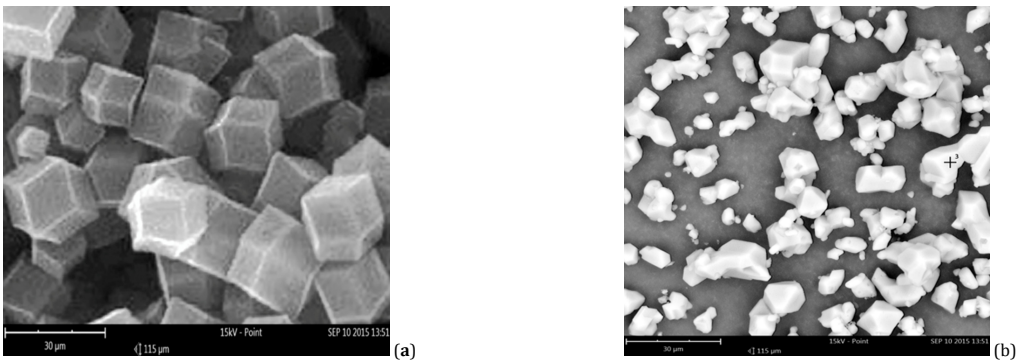

Figure 10. SEM images of the ZIF-8 (a) and MOF-199 (b) samples.

It is interesting to note which additionally to this analysis, high CO_2 adsorption capacity of these solid preparations in this work. This feature is important for potential applications in this area as a gas storage and separation of the same, very important unit operations in the area of engineering.

3.3. Infrared spectroscopy analysis MOF-199 and ZIF-8

FT-IR is a useful method for identifying organic functional groups present in the metal-organic frameworks (MOF's) synthesized intis research (ZIF-8 and MOF-199, see Figure 9). All the vibration bands of IR spectra were in good agreement with the published data on MOF-199 [11].

The IR spectra of the MOF-199 exhibited the strong stretching vibration of carboxylate anions at 1647 cm^{-1}, proving the existence of the reaction of -COOH groups in the 1,3,5-benzenetricarboxylic acid with metal ions. The doublet at 1585 and 1449 cm^{-1} is due to the ν_{asym} (CO_2) and ν_{sym} (CO_2) units. The peak at 1354 cm^{-1} is associated with ν(C=O). The appearance of a broad band at 3500-2700 cm^{-1}indicated the presence of water and -OH groups in the structure of the material. In general, of scale absorption bands in the range 1700-500 cm^{-1} and 1500-1300 cm^{-1} correspond to ν_{asym}(C-O_2) and ν_{sym}(C-O_2) [65]. The other very intense absorption band is centered at 738 cm^{-1} and it was previously assigned in literature [65,66] to ν(C-H) bending mode. In the considered range only the band centered at 505 cm^{-1} is assigned to a vibrational mode directly involving the Cu centre. Following the previous interpretations, [66] this feature is assigned to Cu-O stretching mode.

On the another hand, the infrared spectra of ZIF-8 also all the vibration bands of IR spectra were in good agreement with the published data on ZIF-8 [67-69].

At higher frequency the activated ZIF-8 shows two contributions: the first one centered at 3124 cm^{-1} and the second one in the 3500-3000 cm^{-1} range, ascribable to C-H stretching vibrational modes respectively of the ring and of the methyl group present in the 2-methylimidazole linker. The peak at 1591 cm^{-1} can be assigned as the C-N stretch mode specifically, whereas the intense and convoluted bands at 1510-1380 cm^{-1} are associated with the entire ring stretching [66]. The bands in the spectral region of 1175 - 900 cm^{-1} are for the in-plane bending of the ring while those below 758 cm^{-1} are assigned as out-of-plane bending [67,70]. As expected, clearly, a very intense band at 633 cm^{-1} due to Zn-N stretching mode is clearly observed [57,58,68-70].

3.4. Scanning electron microscope (SEM) micrographs analysis

The scanning electron microscopy of ZIF-8 (see Figure 10a) has a classic morphology and reported in the literature of type rhombic dodecahedron. Performing a more detailed analysis of different micrographs made (not shown here), was established that this material synthesized in this work under the experimental conditions used presents 12 exposed faces (1 1 0) type, analyzed widely and reported in literature [59,60]. From Figure 5, is possible inferred that the size of ZIF-8 samples synthesized were 20-30 μm.

During the taking of the micrographs of ZIF-8 elemental mapping was performed by recording EDX (Energy-dispersive X-ray spectroscopy-not shown here). The results showed a homogeneous distribution of Zn, C, O, and N in ZIF-8 particles, allowing you to check who has successfully synthesized ZIF-8 molecules similar to those reported in the literature characteristic.

In Figure 10b microphotography for MOF-199 prepared in this research is shown. The images reveal tastefully designed octahedral morphology crystals which have a size of about 20-30 microns. I morphology of as-prepared samples MOF-199 was consistent with other SEM images published for this materials [57-61,68-69]. This case also elemental mapping was performed by recording EDX (Energy-dispersive X-ray spectroscopy- not shown here). The results showed a homogeneous distribution of Cu and O in MOF-199 particles, allowing you to check who has successfully synthesized MOF-199 molecules similar to those.

3.5. Adsorption isotherms from aqueous solution of phenols on MOF's

3.5.1. Determination of point of zero charge (pH_{pzc}) and effect of pH

The pH of the solution is an important variable to establish both the active sites of the surface of MOF's and to establish the behavior of this species as adsorbent of phenol and 4-nitrophenol, so it should set the impact that this variable has on the adsorption capacity of these contaminants used as probe molecules. A very interesting measurement that allows establishing this effect on adsorption capacity is the pH of point of zero charge (pH_{pzc}).These measurements allow explain and optimize of adsorption both of phenol and 4-Nitrophenol, on MOF's (ZIF-8 and MOF-199) at different pH ranges (2-12 in this research). Figure 11 illustrates the relationship between solution pH of MOF-199 and ZIF-8, respectively, and the masses for establish of pH of point charge zero (pH_{pzc}). It can be seen that pH_{pzc} of the ZIF-8 particles is around 9.8, this value of pH_{pzc} implies that the surface of the ZIF-8 is positively charged when solution pH is below 9.8, while the surface of ZIF-8 becomes negatively charged at solution pH above 9.8.

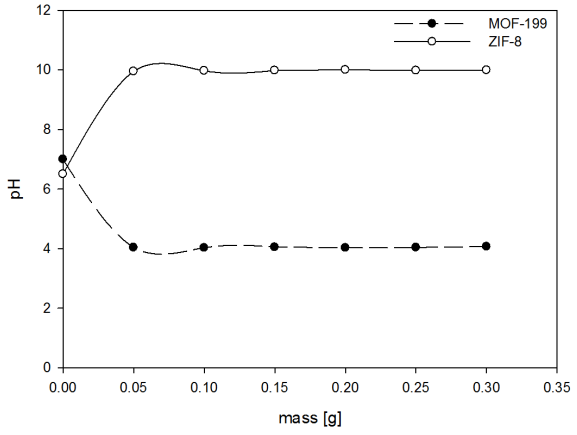

Figure 11. pH_{PZC} graphs of MOFs.

On the other hand a similar analysis can be performed with the results obtained for the pH_{PZC} deteminación for MOF-199 (see Figure 11). To this solid the pH_{PZC} is pH = 4.0, which means that the surface thereof is positively charged when solutions at pH below 4.0 and otherwise when above this value the surface is negatively charged.

The results of the influence of pH in terms of adsorption capacity for phenol and 4-nitrophenol on the ZIF-8 and MOF-199 are shown in Figure 12. In Figure 12a, the results for adsorption for Ph and PNP from aqueous solution on the ZIF-8 is shown specifically. It can be seen from the figure that the maximum adsorption of 4-nitrophenol on ZIF-8 is presented to practically neutral pH, this probably because the surface of the ZIF-8 at this pH is positively charged. Furthermore, it must be noted that the optimum pH for adsorption of phenol is greater than the pH at which the maximum amount adsorbed 4-nitrophenol. This difference can be attributed to different of the following propositions: the first due to a higher pK_a = 9.95 for phenol compared with for 4-nitrophenol that has a pK_a = 7.16. The second: the curves associated with speciation in function of pH of phenolic compounds used in this research. Phenol at low pH is not dissociated, but by increasing the pH to reach a pH around 7 begins to form the phenolate, which causes the solution has negative charges due to this separation, and, moreover, since pH_{PZC} the ZIF-8 is 9.6, allows the phenol and 4-nitrophenol are adsorbed. However PNP have a more acidic than phenol molecule so that it tends to adsorb a greater amount on the ZIF-8 Ph character. Therefore to increase the system pH from neutral to basic, the adsorption of both molecules (Ph and PNP) on ZIF-8 greatly diminished. This can be explained taking into account that the charge density of the ZIF-8 decreases significantly with increasing pH of the solution may occur that can acquire negative charges that create electrostatic repulsion between phenolic type compounds [71,72]. Furthermore, in Figure 12b adsorption behavior of Ph and PNP on MOF-199 at different pH from aqueous solution is shown. The results show that the adsorption of organic molecules such as probe molecules used in this study, when adsorbed on MOF-199 its adsorption capacity also depends on the pH of the solution. Again the maximum amount of adsorption in MOF-199 corresponds to 4-nitrophenol is achieved at a pH around pH = 5, this due mainly because the surface of MOF-199 is positively charged below pH_{PZC} that for MOF-199 corresponds to a pH of 4.0.

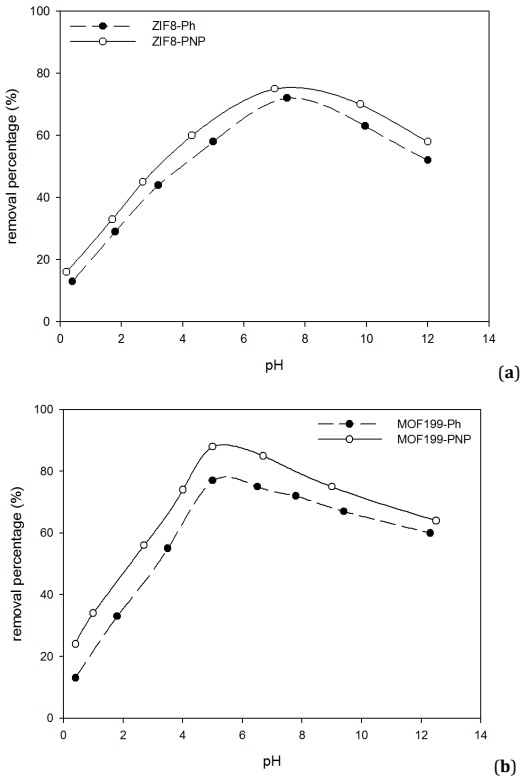

Figure 12. Effect of solution pH on Ph and PNP adsorption on a) ZIF-8 and b) MOF-199.

The maximum amount of adsorption was achieved with 4-nitrophenol molecule to above (pH = 5.0). The difference between the pH of phenol and 4-nitrophenol adsorption, can be attributed to the physicochemical properties of the two compounds and in particular to the difference in the pK_a

Table 5. Equilibrium isotherms constants of Ph on MOF-199 and ZIF-8 at 25.0±0.2 °C.

Adsorbate	Freundlich			Langmuir			Redlich-Peterson				Sips			
	K_F	1/n	R^2	Q_o	b	R^2	k_1	k_2	M	R^2	Q0	Ks	1/ns	R^2
MOF-199 Ph	13.30	0.37	0.94	131.61	0.017	0.99	2.38	0.020	0.98	0.99	136.51	0.016	0.94	0.99
ZIF-8 Ph	8.23	0.31	0.89	55.01	0.022	0.98	1.04	0.011	1.09	0.98	53.00	0.024	1.12	0.98

values: the higher pK_a = 9.95 for phenol compared to the pK = 7.16 for 4-nitrophenol, values that are associated with the acidity of each compound and due to its chemical structure have changes by changing its pH and the adsorbent medium [72].

Adsorption from aqueous solution of phenolic compounds (Ph and PNP) on MOF-199 decreases considerably when the pH is increased from pH = 5: For this instance of MOF-199, present the same behavior as the ZIF-8 presents (pH at which the maximum adsorption capacity is reached) to Basics values. This behavior can be explained if one considers that the pH_{PZC} for MOF-199 particles is around 4.3, and therefore the value of pH_{PZC} means (as discussed for ZIF-8), the surface of the MOF-199 is positively charged when the solution pH is below 4.3, while the surface of MOF-199 is negatively charged in solution pH above 4.3 [72,73].

In summary, it is shown that under the experimental conditions of this study the main factors affecting the adsorption capacity of phenolic compounds used are the pH of the solution affects the surface charge of the solid preparations (MOF-199 and ZIF-8), the degree of ionization and speciation of phenol and 4-nitrophenol (see figures speciation). In this research, the pH ranged between 2 and 12.

During the study of the influence of pH, other variable that can influence on the adsorption capacity MOF's remained constant (for example, contact time (300 min), the dose of adsorbent (5 g/L) and adsorbate concentration (25 mg/L)). Figures 12a and 12b can be concluded that the removal of phenol and *p*-nitrophenol on ZIF-8 and synthesized MOF-199 in this study, was increased with increasing solution pH = 2-7 for phenol in ZIF-8 and then decreases.

Around pH = 7 present, the maximum adsorption capacity of phenol and *p*-nitrophenol for ZIF-8, while for MOF-199 maximum adsorption occurs at pH = 5. It was found that under these experimental conditions, the ZIF-8 adsorbs approximately 65.5% phenol and 77.0% 4-nitrophenol. While the MOF-199 adsorbed on the same conditions already described, approximately 79.55% of phenol and 89.3% of 4-nitrophenol. The dependence of phenol and *p*-nitrophenol removal in the pH of the solution could be explained in terms of both the ZIF-8 and MOF-199 surface charge and species present in the solution of adsorbate.

From Figure 12a and 12b (pH_{pzc}) it can be concluded that the ZIF-8 have a pH_{pzc} equal to 9.8, and therefore the ZIF-8 surface charge is positive at pH < 9.8 whereas at pH > 9.8 the surface charge is negative, while for the MOF-199 have a pH_{pzc} equal to 4.3, this is interpreted as its charge is positive pH < 4.3 whereas at pH > 4.3 the surface charge is negative [74,75].

Now if the pK_a values are analyzed for the two adsorbates that were used in this research the pK_a value of phenol is 9.95 hence below this pH phenol is considered a neutral molecule and above this value is found as anionic species; this interpretation is valid for 4-nitrophenol molecule has pK_a = 7.16 [75].

Thus at low pH values the surface charge is positive and the H^+ ion concentration in solution is high, therefore competition between H^+ and phenol species could occur [14] which cause a low adsorption of phenols by adsorbents, As it has been extensively discussed in the literature by other authors [76].

At pH = 7 where the maximum phenol removal was achieved (and pH = 5 for 4-nitrophenol), the adsorbent surface is negatively charged and neutral phenol species are present in solution. This phenomenon has been explained by some authors using the same type of molecules on other surfaces because, due to weak interactions or the lack them there is no repulsion between phenols and the adsorbent, and their interaction can happen in a free way through π electrons [76,77]. In the particular case of the adsorbate-adsorbent system under study, it is possible that may occur a little strong interactions. Nevertheless, based on the above results, pH value of 7 (for phenol and pH = 5 for 4-nitrophenol) was kept constant in the subsequent experiments to ensure maximum removal of both phenol and *p*-nitrophenol.

Finally, it is interesting to analyze in detail the effect of -NO_2 group in the molecule of 4-nitrophenol; this group within the PNP molecule causes a series of resonant structures that allow the ion H^+ located in the -OH group of the phenol destabilizing molecule and therefore it has a more acidic generate the same molecule phenol , which is reflected in its pK_a (7.16) lower value, this due to the molecule when pH of the solution is increased, it dissociates to form 4-nitrophenolate, which can be seen in curve speciation of according to the following reaction [76-80]:

$$Ar\text{-}OH + H\text{-}OH \rightleftharpoons Ar\text{-}O^- + H_3O^+ \quad (2)$$

Therefore it can provide greater retention amount of this molecule on the prepared adsorbents and particularly adsorbed but the MOF-199 which is 4.3 pH_{pzc}.

In general it can be concluded from the study of variable pH, that the values of around of 7 and 5 are considered to be the best pH for maximum removal of Ph and PNP, for ZIF-8 and MOF-199 respectively [76-79].

The decrease in removal percentage of phenols with increased pH values may be due to the increase in magnitude of negative charges on Ph or PNP and which also affects the PZC both ZIF-8 as the MOF-199, which generate repulsion between adsorbate-adsorbent so that the amounts of Ph or PNP adsorbed then decrease, as explained by Al-Mutairi [76] who reported 93.6% maximum removal percentage of 2,4-dinitrophenol by other material at optimum pH value of 4 and constant conditions of 100 mg/L initial concentration, 0.5 g/L dose, 313 K temperature and 5 h contact time.

3.5.2. Adsorption isotherms from aqueous solution: phenols-MOFs system-

In order to perform a detailed study of the adsorption of phenol molecules on MOF's with the results obtained in this research they were applied to six model system and were fitted with data for both the Ph as PNP obtained in experiments when placed in contact on MOF-199 and ZIF-8 under the conditions established in this investigation. For each model, the respective parameters are calculated and also the adjustment coefficient R^2, which was used as criteria to establish which model, is better and adjusted to the system under study. Table's 5a and 5b shows the results calculated with the results found in each experiments adsorption from aqueous solution with the phenols-MOF's systems. Figure 13a and 13b show the respective adsorption isotherms from aqueous solution systems. In each of the figures they are plotted the curves for respective models used in this study. According to the previous paragraph, the best fit will be set according to the value of R^2, this means that the closer to the unit.

Table 6. Equilibrium isotherms constants of PNP on MOF-199 and ZIF-8 at 25.0±0.2 °C.

Adsorbate	Freundlich			Langmuir			Redlich-Peterson				Sips			
	K_F	1/n	r^2	Q_o	b	r^2	k_1	k_2	M	r^2	Q0	Ks	1/ns	r^2
MOF-199 PNP	21.18	0.36	0.91	203.29	0.015	0.97	2.41	0.004	1.19	0.98	194.68	0.017	1.11	0.97
ZIF-8 PNP	7.54	0.33	0.93	59.17	0.020	0.98	1.14	0.018	1.01	0.98	61.80	0.018	0.91	0.98

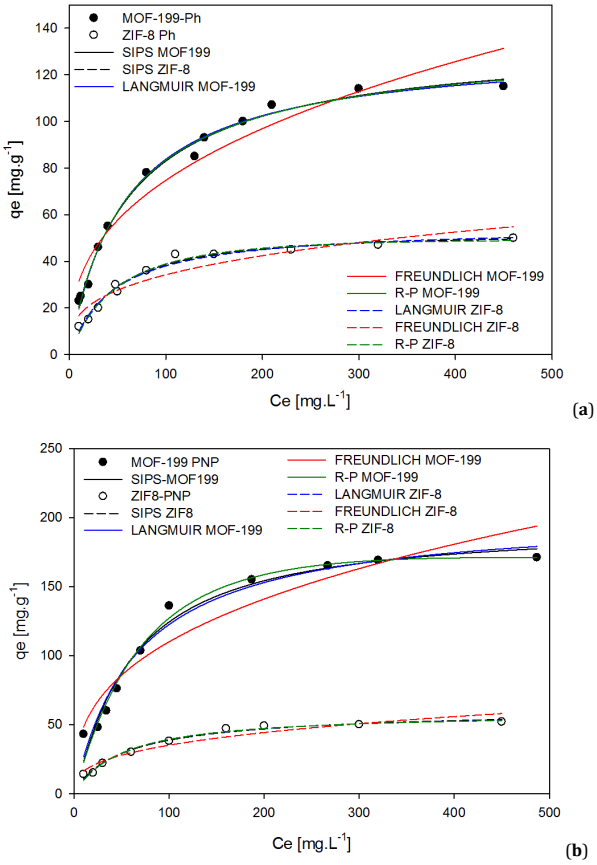

Figure 13. Comparison of different isotherm models for Ph and PNP adsorption on MOF-199 and ZIF-8. a) MOF-199/ZIF-8-Ph and b) MOF199/ZIF-8 PNP. Ajusted to: Langmuir, Freundlich, Sips and Redlich-Peterson (R-P).

Between these models used in this work of Langmuir was applied, [77] which assumes that the adsorption occurs as a monolayer on a homogeneous surface containing limited adsorption sites. Thus once an adsorption site has been occupied, it is not possible to adsorb other adsorbate. This model is applied, because to it is a model is widely used in the scientific literature for interpretation in studies on liquid-solid interactions.

Therefore, a saturated adsorption capacity (i.e., a maximal adsorption capacity, q_{max}) is expected in Langmuir isotherm that is described according to the equation that shows itself in the Table 5 and 6.

Adsorption isotherms of phenolic compounds on MOFs were studied and modeled using were two isotherm models with two parameters and two isotherm models with more than two-parameter. An excellent prediction in all the studied concentration range can be obtained by the three-parameter equations. In the literature, the researchers generally compare the equations with three parameters with the two-parameter equations of Langmuir and Freundlich, and they generally concluded from their studies that the equations with more than two parameters are always better than those with two parameters.

The model of Freundlich diverges with the experimental results for the higher values of equilibrium concentrations. Thus, in agreement with other authors, it is suggested that the Freundlich model is only valid at low equilibrium concentrations of the adsorbate in solution. Sips circumvent the limitation of the rising adsorbate concentration associated with the Freundlich isotherm model.

Recognizing the problem of the continuing increase in the adsorbed amount with an increase in concentration in the Freundlich equation, Sips proposed an equation similar in form to the Freundlich equation, but it has a finite limit when the concentration is sufficiently high. The Sips isotherm equation is sometimes called the Langmuir-Freundlich equation in the literature because it has the combined form of Langmuir and Freundlich [81-83]

From the results shown in Table 5 and 6 must be emphasized that, according to the obtained values of r^2, systems have also a good fit are phenol's-MOF's systems using Redlich-Peterson model [80], although a slight deviation occurs in setting the graphics shown in the Figure 13.

3.5.3. Kinetic analysis of the results of the system phenol's-MOFs

It is very interesting to perform the kinetic study of the adsorbate in the adsorption-adsobente-MOF'S phenols system because it provides adequate information on the mechanism of absorption of solute in an adsorbent.

Table 7. Pseudo-first order, Elovich's, pseudo-second order and intra-particle diffusion kinetic model parameters for the adsorption of Ph and PNP on MOF-199 and ZIF-8 into an aqueous solution of initial concentration 500 ppm.

	Ph-MOF-199	PNP- MOF-199	Ph-ZIF-8	PNP- ZIF-8
Pseudo-first order model				
q_e(mg/g)	58.34	67.54	50.16	54.56
k_1 (min^{-1})	0.021	0.015	0.027	0.018
r^2	0.989	0.978	0.987	0.967
Elovich's equation				
a (mg/(g min))	2.23	3.28	1.87	2.13
1/b (mg/g)	0.139	0.123	0.15	0.189
r^2	0.923	0.935	0.932	0.937
Pseudo-second order model				
k' (g/(mg min))	5.43×10^{-2}	2.23×10^{-2}	3.54×10^{-2}	3.34×10^{-2}
q_e (mg/g)	124.32	136.76	101.54	112.23
r^2	0.999	0.999	0.999	0.999
Intra-particle difussion model				
K_{int1}(mg/g $min^{1/2}$)	111.22	120.21	96.43	90.32
r_1^2	0.955	0.925	0.906	0.897
K_{int2}(mg/g $min^{1/2}$)	45.56	53.65	40.34	42.29
C^2	76.32	82.76	77.34	73.12

This is why to establish the kinetics of Ph and PNP on MOF-199 and ZIF-8 and four kinetic models applied to analyze the results obtained in this investigation. The first model was the pseudo first order equation of Lagergren [84] it is one of the most widely used for adsorption of solute from a liquid. Once reorganized and linearized, reads: The pseudo first-order equation is often described as follows Equation 3:

$$\ln (q_e - q_t) = \ln q_e - k_1 t \quad (3)$$

where t (min) is the mixing time and k_1 (min^{-1}) is the pseudo first order rate constant.

The second model applied is an equation developed by Roginsky-Zeldowitsch [84], which was widely used by researchers to study the adsorption of solutes across the floor. Then this equation was modified by others authors and their applicability was extended and today received the name by which he is known: Elovich equation [85,86]. It is also the equation Elovich has also been successfully used to describe the adsorption of pollutants from aqueous solutions in recent years [86], and can be expressed as follows equation 4:

$$q_t = (\ln ab) + \frac{1}{b}\ln(t) \quad (4)$$

where a is the initial adsorption rate (mg/(g min)), and the parameter 1/ b (mg/g) is related to the number of sites available for adsorption. If this equation applies, it should lead to a straight line by plotting q_t as a function of ln t.

The third model applied was Pseudo second-order model. The pseudo-second-order equation may be expressed in the following equation 5:

$$\frac{t}{q_t} = \frac{1}{k' q_e^2} + \frac{1}{q_e} t \quad (5)$$

in which q_t and q_e have the same meaning as before, and k' is the corresponding kinetic constant (g/(mg min)). If a plot of t/q_t versus t is performed, and if the model is true that describes this equation (Equation 5), a straight line of slope $1/q_e$ must be obtained. Table 7 shows the parameters derived from the application of pseudo-first order equation (k_1) and ke, Elovich equation (a and b), and the pseudo second order kinetic model (k' and q_e). For each case, the corresponding correlation coefficients, r^2, are given. For each case, the corresponding correlation coefficients, r^2, are given. Neither Equation (3) or (4) may be adjusted properly adsorption data, since the values of r^2 corresponding to equation (4) that are found between 0.92 to 0.93 for all MOF's investigated, whereas r^2 Equation (3) they are around 0.98, with low value compared to the results obtained by applying the models pseudo-second order. However, correlation coefficients r^2 equal to unity were found for the MOF's by application of Equation (5), see Figure 14a. In this model, a pseudo second-order model for all the investigated materials can very satisfactorily approximate the sorption kinetics. Such a finding is also in good agreement with previous studies [87].

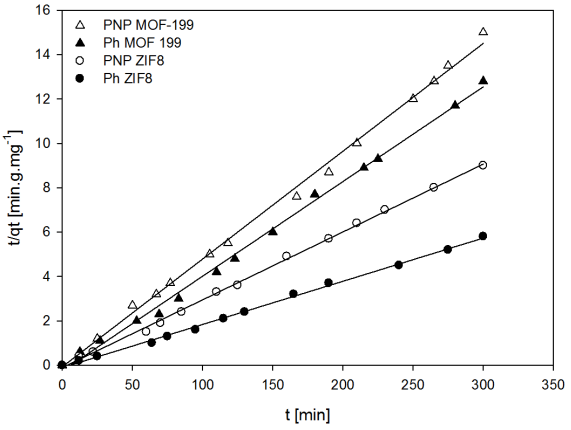

Figure 14. Application of pseudo second-order model to data experimental for phenol's-MOF'S system.

The last model employed was Intra-particle diffusion (IPD). In this model developed by Weber and Morris [88], McKay and Poots [89], the initial rate of intra-particle diffusion is calculated by linearization of equation which is shown below.

The overall adsorption process may indeed be controlled either by one or more steps, e.g. film or external diffusion, pore diffusion, surface diffusion and adsorption on the pore surface, or a combination of more than one step. In a rapidly stirred batch, the diffusive mass transfer can be related by an apparent diffusion coefficient, which will fit the experimental sorption rate data. Generally, a process is diffusion-controlled if its rate depends on the rate at which components diffuse towards one another. The possibility of intra-particle diffusion was explored by using the intra-particle diffusion model [89], according to which the amount adsorbed at time t, q_t, reads:

$$q_t = k_{id} . t^{1/2} + C \quad (6)$$

where k_{id} is the intra-particle diffusion rate constant (mg/(g.$min^{1/2}$)), and C (mg/g) is a constant related to the

Table 8. Thermodynamic parameters of phenol and *p*-nitrophenol adsorption by MOF-199 and ZIF-8.

System	Temperature (K)	-ΔG° (kJ/mol)	ΔH° (kJ/mol)	-ΔS° (kJ/mol)
Ph-MOF-199	298	26.45	19.46	5.47
	313	28.32		
	333	33.56		
PNP-MOF-199	298	38.23	24.86	6.78
	313	43.78		
	333	48.12		
Ph-ZIF-8	298	21.32	13.67	3.23
	313	24.76		
	333	29.45		
PNP-ZIF-8	298	24.12	15.34	4.34
	313	27.34		
	333	36.98		

thickness of the boundary layer: the larger is the value of C, the greater is the boundary layer effect [89,90]. If the so-called Weber-Morris [87] plot of q_t versus $t^{1/2}$ gives a straight line, then the sorption process is controlled by intra-particle diffusion only. However, if the data exhibit multi-linear plots, then two or more steps influence the sorption process. It is assumed that the external resistance to mass transfer surrounding the particles is significant only in the early stages of adsorption: this is represented by the first sharper portion. The second linear portion is the gradual adsorption stage with controlling intra-particle diffusion [89-91].

3.5.4. Adsorption thermodynamics

Finally, evaluate the thermodynamic parameters allow to study whether or not the process is spontaneous during the adsorption process; For this reason, experiments at different temperatures (298, 313 and 328 K) were performed. With the experiment results the following variables were calculated: Gibbs free energy (ΔG°), enthalpy (ΔH°) and entropy change (ΔS°) of the adsorption process with the following equations:

$$\ln K_L = \frac{\Delta S^o}{R} - \frac{\Delta H^o}{R.T} \quad (7)$$

where K_L is the Langmuir constant, (ΔG°) is the Gibbs free energy change, (ΔH°) is the enthalpy change, the entropy change (ΔS°), T is the temperature (K) and R is the gas constant (8.314 J/mol K).

Thermodynamic parameters for Ph and PNP adsorption, onto the MOF-199 and ZIF-8 adsorbents were listed in Table 8.

The values obtained for the change in free energy (ΔG°) is negative character which is thermodynamically interpreted assuming that the adsorption of phenol-MOF's systems is spontaneous. These values change according to systems: the PNP-MOF and Ph-ZIF-8 system is within the range of 48.12 to 26.46 kJ/mol, respectively, while for the PNP-ZIF-8 and Ph-ZIF-8 system the value of the free energy Gibbs (ΔG°) is between 36.98 and 21.32 kJ/mol, respectively.

Under the experimental conditions of our research, with increasing temperature the free energy Gibbs (ΔG°) increase, which means that these MOF's have the ability to adsorb more phenols at higher temperatures which makes applications viable industrial character.

On the other hand the positive character of the enthalpy (ΔH°) is showing that the phenol adsorption MOF's are endothermic, with rates ranging between 24.86 kJ/mol for the PNP-MOF-199 system and 13.67 kJ/mol for Ph-ZIF-8. The magnitude of the type of interaction gives an idea of the type of interaction that occurs between the adsorbate and the adsorbent: when it is in a range of 2-20 kJ/mol talking about physical interactions, whereas when they are greater than 50 kJ/mol he talks about chemical type interactions.

For this work the interactions are of the physical type, which is good, because once phenols molecules are retained, it becomes easier to remove the MOF network.

Finally entropic values are between 3.23 and 6.78 kJ/mol for Ph-ZIF-8 and the PNP-MOF-199 were obtained respectively. Negative values for entropy (ΔS°) values suggest that the adsorbate molecules probably have a less random motion in the adsorbate-adsorbent interface and hence tend to generate an organization in said interface during the adsorption process.

4. Conclusions

In this present study, we successfully synthesized, MOF-199 and ZIF-8 and demonstrated their capability as an adsorbent to remove phenol and *p*-nitrophenol from aqueous solutions. The adsorption of Ph and PNP on MOF's could be attributed to several chemical interactions such as the affinity of $-NO_2$ of phenols to copper of MOF-199 and zinc of ZIF-8 respectively, as well as the π-π interaction between the phenol compounds and of MOF's. These affinities also enabled to demonstrate that MOFs obtained on this research possess a high selectivity towards Ph and PNP during the adsorption. The findings in this study revealed that MOF-199 and ZIF-8 can be effective adsorbents to remove Ph and PNP, a highly toxic pollutant, from aqueous solutions. In addition the gas phase studies show that MOF's structures can be ideal for storing CO_2. Finally, thermodynamic studies show that phenols-MOF's system adsorption kinetics follow a pseudo-second order and the adsorption phenomenon is spontaneous according to the values obtained for the Gibbs free energy.

Acknowledgements

The authors would like to thank the frame agreement between the Universidad Nacional de Colombia and Universidad de los Andes (Colombia). Additionally, the authors acknowledge fund Basic Science of Faculty of Sciences and the Vice-rectory of Research at the University of the Andes (Colombia) for partially financing this research. Also, a thanks special to project 3580 of Bank of the Republic for its financial support.

References

[1]. Shen, H. M.; Zhua, G. Y.; Yua, W. B.; Wua, H. K.; Jib, H. B.; Shia, H. X. Shea, Y. B.; Zheng, Y. F. *Appl. Surf. Sci.* **2015**, *356*, 1155-1167.
[2]. Arasteh, R.; Masoumi, M.; Rashidi, A. M.; Moradi, L.; Samimi, V.; Mostafavi, S. T. *Appl. Surf. Sci.* **2010**, *256*, 4447-4455.
[3]. Liu, W.; Jiang, X. Y.; Chen, X. Q. *Appl. Surf. Sci.* **2014**, *320*, 764-771.
[4]. Ofomaja, A. E. Unuabonah, E. I. *Carbohyd. Polym.* **2011**, *83*, 1192-1200.
[5]. Cotoruelo, L. M.; Marques, M. D.; Diaz, F. J.; Rodriguez-Mirasol, J.; Rodriguez, J. J.; Cordero, T. *Chem. Eng. J.* **2012**, *184*, 176-183.
[6]. Sarkar, B.; Xi, Y. F.; Megharaj, M.; Krishnamurti, G. S. R.; Naidu, R. *J. Colloid. Interf. Sci.* **2010**, *350*, 295-304.
[7]. Han, S.; Zhao, F.; Sun, J.; Wang, B.; Wei, R. Y.; Yan, S. Q. *J. Magn. Magn. Mater.* **2013**, *341*, 133-137.

[8]. Isichei, T. O.; Okieimen, F. E. *Environ. Pollut.* **2014**, *3*, 99-111.
[9]. Ahmad, F.; Daud, W. M. A. W.; Ahmad, M. A.; Radzi, R. *Chem. Eng. J.* **2011**, *178*, 461-467.
[10]. Xue, G. H.; Gao, M. L.; Gu, Z.; Luo, Z. X.; Hu, Z. C. *Chem. Eng. J.* **2013**, *218*, 223-231.
[11]. Sarkar, B.; Megharaj, M.; Xi, Y. F.; Naidu, R. *Chem. Eng. J.* **2012**, *185*, 35-43.
[12]. Sun, Y. Y.; Zhou, J. B.; Cai, W. Q.; Zhao, R. S.; Yuan, J. P. *Appl. Surf. Sci.* **2015**, *345*, 897-903.
[13]. Liu, B. J.; Yang, F.; Zou, Y. X.; Peng, Y. *J. Chem. Eng. Data.* **2014**, *59*, 1476-1482.
[14]. Adam, O. E. A. A.; Al-Dujaili, A. H. *J. Chem.* **2013**, 1-8.
[15]. Park, Y.; Ayoko, G. A.; Kurdi, R.; Horvath, E.; Kristof, J.; Frost, R. L. *J. Colloid. Interf. Sci.* **2013**, *406*, 196-208.
[16]. Bastami, T. R.; Entezari, M. H.; *Chem. Eng. J.* **2012**, *210*, 510-519.
[17]. Rivera-Utrilla, J.; Sanchez-Polo, M.; Gomez-Serrano, V.; Alvarez, P. M.; Alvim-Ferraz, M. C. M.; Dias, J. M. *J. Hazard. Mater.* **2011**, *187*, 1-23.
[18]. Entezari, M. H.; Bastami, T. R. *J. Hazard. Mater.* **2006**, *137*, 959-964.
[19]. Canizares, P.; Lobato, J.; Paz, R.; Rodrigo, M. A.; Saez, C. *Water Res.* **2005**, *39*, 2687-2703.
[20]. Shen, S. F.; Kentish, S. E.; Stevens, G. W. *Sep. Purif. Technol.* **2012**, *95*, 80-88.
[21]. Praveen, P.; Loh, K. C. *J. Membr. Sci.* **2013**, *437*, 1-6.
[22]. Peretti, S. W.; Tompkins C. J.; Goodall, J. L.; Michaels, A. S. *J. Membr. Sci.* **2002**, *195*, 193-202.
[23]. Yao, Y. X.; Li, H. B.; Liu, J. Y.; Tan, X. L; Yu, J. G.; Peng, Z. G. J. *Nanomater.* **2014**, 1-9.
[24]. Zhang, B.; Li, F.; Wu, T.; Sun, D. J.; Li, Y. *J. Colloid. Surf. A.* **2015**, *464*, 78-88.
[25]. Gimeno, O.; Carbajo, M.; Beltran, F. J.; Rivas, F. J. *J. Hazard. Mater.* **2005**, *119*, 99-108.
[26]. Ksibi, M.; Zemzemi, A.; Boukchina, R. *J. Photochem. Photobiol. A.* **2003**, 159, 61-70.
[27]. Erdem, M.; Yuksel, E.; Tay, T.; Cimen, Y.; Turk, H. *J. Colloid. Interf. Sci.* **2009**, *333*, 40-48.
[28]. Koubaissy, B.; Joly, G.; Batonneau-Gener, I.; Magnoux, P. *Ind. Eng. Chem. Res.* **2011**, *50*, 5705-5713.
[29]. Huang, J. H.; Yan, C.; Huang, K. L *J. Colloid. Interf. Sci.* **2009**, *332*, 60-64.
[30]. Lin, K. Y. A.; Yang, H.; Petit, C.; Hsu, F. H. *Chem. Eng. J.* **2014**, *249*, 293-301.
[31]. Stock, N.; Biswas, *S. Morphol. Compos. Chem. Rev.* **2011**, *112*, 933-969.
[32]. Janiak, C.; Vieth, J. K. *New J. Chem.* **2010**, *34*, 2366-2388.
[33]. Mueller, U.; Schubert, M.; Teich, F.; Puetter, H.; Schierle-Arndt, K.; Pastre, J. *J. Mater. Chem.* **2006**, *16*, 626-636.
[34]. Yoon, J. W.; Jhung, S. H.; Hwang, Y. K.; Humphrey, S. M.; Wood, P. T.; Chang, J. S. *Adv. Mater.* **2007**, *19*, 1830-1834.
[35]. Li, J. R.; Ma, Y.; McCarthy, M. C.; Sculley, J.; Yu, J.; Jeong, H. K.; Balbuena, P. B.; Zhou, H. C. *Coord. Chem. Rev.* **2011**, *255*, 1791-1823.
[36]. Li, J. R.; Kuppler, R. J.; Zhou, H. C. *Chem. Soc. Rev.* **2009**, *38*, 1477-1504.
[37]. Lee, J.; Farha, O. K.; Roberts, J.; Scheidt, K. A.; Nguyen, S. T.; Hupp, J. T. *Chem. Soc. Rev.* **2009**, *38*, 1450-1459.
[38]. Corma, A.; García, H.; Xamena, F. X. *Chem. Rev.* **2010**, *110*, 4606-4655.
[39]. Gascon, J.; Corma, A.; Kapteijn, F.; Xamena, F. X. *ACS. Catal.* **2013**, *3*, 361-378.
[40]. Horcajada, P.; Chalati, T.; Serre, C.; Gillet, B.; Sebrie, C.; Baati, T.; Eubank, J. F.; Heurtaux, D.; Clayette, P.; Kreuz, C.; Chang, J. S.; Hwang, Y. K.; Marsaud, V.; Bories, P. N.; Cynober, L.; Gil, S.; Ferey, G.; Couvreur, P.; Gref, R. *Nat. Mater.* **2010**, *9*, 172-178.
[41]. Qiu, L. G.; Li, Z. Q.; Wu, Y.; Wang, W.; Xu, T.; Jiang, X. *Chem. Commun.* **2008**, 3642-3644.
[42]. Ke, F.; Qiu, L. G.; Yuan, Y. P.; Peng, F. M.; Jiang, X.; Xie, A. J.; Shen, Y. H.; Zhu, J. F. *J. Hazard. Mater.* **2011**, *196*, 36-43.
[43]. Li, L.; Li, J. C.; Rao, Z.; Song, G. W.; Hu, B. *Desalination. Water. Treat.* **2014**, *52*, 7332-7338.
[44]. Tranchemontagne, D. J.; Hunt, J. R.; Yaghi, O. M. *Tetrahedron* **2008**, *64*, 8553-8557.
[45]. Britt, D.; Tranchemontagne, D.; Yaghi, O. M. *Proc. Natl. Acad. Sci.* **2008**, *105*, 11623-11627.
[46]. Nguyen, L. T.; Nguyen, T. T.; Nguyen, K. D.; Phan, N. T. *Appl. Catal. A.* **2012**, *425*, 44-52.
[47]. Rowsell, J. L.; Yaghi, O. M. *J. Am. Chem. Soc.* **2006**, *128*, 1304-1315.
[48]. Li, L.; Yao, J.; Xiao, P.; Shang, J.; Feng, Y.; Webley, P. A.; Wang, H. *Colloid. Polym. Sci.* **2013**, *291*, 2711-2717.
[49]. Moellmer, J.; Celer, E. B.; Luebke, R.; Cairns, A. J.; Staudt, R.; Eddaoudi, M.; Thommes, M. *Micropor. Mesoporr Mat.* **2010**, *129*, 345-353
[50]. Barcia, P. S.; Guimarães, D.; Mendes, P. A. P.; Silva, J. A. C.; Guillerm, V.; Chevreau, H.; Serre, C.; Rodrigues, A. *Micropor. Mesopor. Mat.* **2011**, *139*, 67-73.
[51]. Francesc, X.; Xamena, F. X.; Abad, A.; Corma, A.; Garcia, H. *J. Catal.* **2007**, *250*, 294-298.
[52]. Hosny, M. N. *J. Therm. Anal. Calorim.* **2015**, *122*, 89-95.
[53]. Cieplak, P.; Bayly, S. C. I.; Gould, I. R.; Merz, Jr. K. M.; Ferguson D. M.; Spellmeyer, D. C.; Fox, T.; Caldwell, J. W.; Kollman. P. A. *Am. Chem. Soc.* **1995**, *117*, 5179-5197.
[54]. Thommes, M.; Cychosz, K. A.; Neimark, A. V. Advanced physical adsorption characterization of nanoporous carbons. In: Tascón, J. M. D. (ed.) Novels Carbons Adsorbent. Elsevier, Great Britain, 2012.
[55]. Rouquerol, J.; Llewellyn, P.; Rouquerol, F. Is BET equation applicable to microporous adsorbents? In: P. Lewelling, F. Rodriguez-Reinoso, J. Rouquerol, N. Seaton, editors. Characterization of porous solids VII. Amsterdam: Elsevier, Stud. Surf. Sci. Catal., 2007.
[56]. Park, K. H.; Balathanigaimani, M. S.; Shim, W. G.; Lee, J. W.; Moon, H. *Microporous. Mesoporous. Mater.* **2010**, *127*, 1-8.
[57]. Chen, R; Yao, J.; Gu, Q.; Smeets, S.; Baerlocher, C.; Gu, H.; Zhu, D.; Morris, W.; Yaghi, O. M.; Wang, H. *Chem. Commun.* **2013**, *49*, 9500-9502.
[58]. Fairen-Jimenez, D.; Moggach, S. A.; Wharmby, M. T.; Wright, P. A.; Parsons, S.; Duren, T. *J. Am. Chem. Soc.* **2011**, *133*, 8900-8902.
[59]. Danaci, D.; Singh, R.; Xiao, P.; Webley, P. A. *Chem. Eng. J.* **2015**, *280*, 486-493.
[60]. Garrido, J.; Linares-Solano, A.; Martín Martínez, J. M.; Molina-Sabio, M.; Rodríguez-Reinoso, F.; Torregrosa, R. *Langmuir* **1987**, *3*, 76-81.
[61]. Brunauer, S.; Emmett, P. H.; Teller, E. *J. Am. Chem. Soc.* **1938**, *60*, 309-319.
[62]. Landers, J.; Gor, G. Y.; Neimark, A. V. *Colloids Surf., A: Physicochem. Eng. Aspects* **2013**, *437*, 3-32.
[63]. Dubinin, M. M.; Astakhov, V. A. *Biol. Bull. Acad. Sci. USSR.* **1971**, *20*, 3-7.
[64]. Li, G.; Lan, J.; Liu, J.; Jiang, G. *J. Colloid Interface Sci.* **2013**, *405*, 164-170.
[65]. Bordiga, S.; Regli, L.; Bonino, F.; Groppo, E.; Lamberti, C.; Xiao, B.; Wheatley, P. S.; Morris, R. E.; Zecchina, A. *Phys. Chem. Chem. Phys.* **2007**, *9*, 2676-2685.
[66]. Lin, K. S.; Adhikari, A. K.; Ku, C. N.; Chiang, C. L.; Kuo, H. *Int. J. Hydrogen Energy* **2012**, *37*, 13865-13871.
[67]. Cravillon, J.; Münzer, S.; Lohmeier, S. J.; Feldhoff, A.; Huber, K.; Wiebcke, M. *Chem. Mater.* **2009**, *21*, 1410-1412.
[68]. Yue, Y.; Binder, A. J.; Song, R.; Cui, Y.; Chen, J.; Hensley, D. K.; Dai, S. *Dalton Trans* **2014**, *43*, 17893-17898.
[69]. Fracaroli, A. M.; Furukawa, H.; Suzuki, M.; Dodd, M.; Okajima, S.; Gándara, F.; Reimer, J. A.; Yaghi, O. M. *J. Am. Chem. Soc.* **2014**, *136*, 8863-8866.
[70]. Pan, Y. C.; Liu, Y. Y.; Zeng, G. F.; Zhao, L.; Lai, Z. P. *Chem. Commun.* **2011**, *47*, 2071-2073.
[71]. Jian, M.; Liu, B.; Zhang, G.; Liu, R.; Zhang, X. *Colloids Surf., A: Physicochemical Eng. Aspects* **2015**, *465*, 67-76.
[72]. Diaz-Flores, P. E.; Lopez-Urı, F.; Terrones, M.; Rangel-Mendez, J. R. *J. Colloid Interface Sci.* **2009**, *334*, 124-131.
[73]. Abdel-Ghani, N. T.; El-Chaghaby, G. A.; Helal, F. S. *J. Adv. Res.* **2015**, *6*, 405-415.
[74]. Ahmed, M. J.; Theydan, S. K. *Ecotoxicol. Environ. Saf.* **2012**, *84*, 39-45.
[75]. Ahmed, M. J.; Theydan, S. K.; Mohammed, A. H. A. *J. Engineering* **2012**, *18*, 1-13.
[76]. Al-Mutairi, N. Z. *Desalination* **2010**, 2*50*, 892-901.
[77]. Langmuir, I. *J. Am. Chem. Soc.* **1916**, *38*, 2221-2295.
[78]. Freundlich, H. M. F. Z. Phys. Chem. **1906**, *57*, 385-470.
[79]. Uddin, M. T.; Islam, M. S.; Abedin, M. Z. *J. Eng. Appl. Sci.* **2007**, *2*, 121-128.
[80]. Radke, C. J.; Prausnitz, J. M. *Ind. Eng. Chem. Fund.* **1972**, *11*, 445-451.
[81]. Hamdaoui, O.; Naffrechoux, E. *J. Hazard. Mater.* **2007**, *147*, 401-411.
[82]. Humpola, P., Odetti, H.; Moreno-Piraján, J. C.; Giraldo, L. Adsorption 2016, 22, 23-31.
[83]. Duong, D. Do. In Adsorption Analysis: Equilibria and Kinetics. Practical Approaches of Pure Component Adsorption Equilibria. Imperial College Press, 1998.
[84]. Lagergren, S. K. *Sven. Vetenskapsakad. Handl*. **1898**, *24*, 1-39.
[85]. Zeldowitsch, J. *Acta Physicochim. U. R. S. S.* **1934**, *1* 364-449.
[86]. Allen, J. A.; Scaife, P. H. *Aust. J. Chem.* **1966**, *19*, 2015-2023.
[87]. Fierro, V.; Torné-Fernández, V.; Montané, D.; Celzard, A. *Microporous. Mesoporous. Mater.* **2008**, *111*, 276-284.
[88]. Weber, W. J.; Morris, J. C. *ASCE J. Sanit. Eng. Div.* **1963**, *89*, 31-42.
[89]. McKay, G.; Poots, V. J. P. *J. Chem. Technol. Biotechnol.* **1980**, *30*, 279-292.
[90]. Crank, J. *Oxford Clarendon* **1965**, *84*, 84-88.
[91]. Asfour, H. M.; Nassar, M. M.; Fadali, O. A.; El-Geundi, M. S. *J. Chem. Technol. Biotechnol.* **1985**, *35*, 28-35.